Carboxylated Multiwall Carbon Nanotube-Reinforced Thermotropic Liquid Crystalline Polymer Nanocomposites

Sang Ki Park,[1] Seong Hun Kim,[1] Jin Taek Hwang[2]

[1]*Department of Fiber and Polymer Engineering, Hanyang University, Seoul 133-791, Korea*
[2]*E-Polymer, 110-15, Yanggam-Myon, Hwasung-Si, Kyunggi-Do 445-931, Korea*

Received 19 October 2007; accepted 6 January 2008
DOI 10.1002/app.28137
Published online 28 March 2008 in Wiley InterScience (www.interscience.wiley.com).

ABSTRACT: Thermotropic liquid crystalline polymer (TLCP) nanocomposites reinforced with carboxylated multiwall carbon nanotube (c-MWCNT) were prepared through melt compounding in a twin screw extruder. The thermal stability of TLCP/c-MWCNT nanocomposites increased with even a small amount of c-MWCNT added. The rheological properties of the TLCP/c-MWCNT nanocomposites were depended on the c-MWCNT contents. The contents of c-MWCNT have a slight effect on the complex viscosity of TLCP/c-MWCNT nanocomposites due to the high-shear thinning of TLCP. The storage modulus of TLCP/c-MWCNT nanocomposites was increased with increasing c-MWCNT content. This result can be deduced that the nanotube–nanotube interactions were more dominant, and some interconnected or network-like structures were formed in the TLCP/c-MWCNT nanocomposites. Incorporation of very small amount of c-MWCNT improved the mechanical properties of TLCP/c-MWCNT nanocomposites, and this was attributed to the reinforcement effect of c-MWCNT with high aspect ratio and their uniform dispersion through acid treatment in the TLCP matrix. © 2008 Wiley Periodicals, Inc. J Appl Polym Sci 109: 388–396, 2008

Key words: thermotropic liquid crystalline polymer; carbon nanotube; nanocomposites; reinforcement

INTRODUCTION

Polymer nanocomposites have attracted considerable interest in the polymer materials industry because of their outstanding properties such as excellent electrical and mechanical properties. In the recent years, various attempts have been made to develop high-performance polymer nanocomposites, using the benefits of nanoscience and nanotechnology, including the introduction of nanoscaled reinforcements into polymer matrix. Because the discovery of carbon nanotubes (CNT) by Iijima[1] in 1991, CNT has been considered as an ideal reinforcement to fabricate high-performance polymer nanocomposites because of its excellent physical properties, such as extremely high mechanical strength, electrical, and thermal conductivity.[2–6]

Uniform dispersion of CNTs in the polymer matrix and strong interfacial interaction, leading to efficient load transfer from polymer matrix to the CNTs, are the key factor to produce high-performance polymer/CNT nanocomposites.[7] In general, chemical functionalization of CNT has accepted as an effective method for uniform dispersion of CNT in the polymer matrix and for improving the interfacial adhesion between CNT and polymer matrix by reducing agglomeration of CNT and improvement in compatibility.[8–10] There are two methods to functionalize the surface of CNT; the one is attachment of molecules through the noncovalent bond; the other is attachment of functional groups to the walls of CNT through the covalent bond. The attachment of functional group to the wall of CNT through the covalent bond can be occurred by concentrated acid or their mixture, forming carboxylic acid group on the surface of CNT. In addition, the presence of carboxylic acid groups on the surface of CNT can offer various chemical reactions.[11]

The polymer matrix used in this study to fabricate high-performance polymer/CNT nanocomposites was thermotropic liquid crystalline polymer (TLCP). TLCPs have been considered as high-performance engineering plastics because of their high mechanical properties, excellent dimensional stability, and good processability.[12–15] Up to now, various kinds of thermoplastic materials have studied to fabricate polymer/CNT nanocomposites by melt-compounding process.[16–23] However, there are little attempts to

Correspondence to: S. H. Kim (kimsh@hanyang.ac.kr).
Contract grant sponsor: Ministry of Commerce, Industry, and Energy; contract grant number: 10020777.
Contract grant sponsor: Ministry of Education and Human Resources Development (Brain Korea 21 program).

improve dispersion of CNT in the engineering plastic such as TLCP and to fabricate the TLCP/CNT nanocomposites by melt compounding. In addition, the study on TLCP/CNT nanocomposites has not yet been reported in the literature.

In this research, the TLCP nanocomposites reinforced with CNT were prepared by melt compounding at various CNT contents. The carboxylated multiwall carbon nanotube (c-MWCNT) treated with mixture of sulfuric acid and nitric acid was used to improve the dispersion of CNTs in the TLCP matrix and the interfacial adhesion between CNT and TLCP matrix. In addition, the amount of c-MWCNT incorporated into the TLCP was lowered to 0.01–0.2 wt % to obtain uniform and homogeneous dispersion of c-MWCNT in the TLCP matrix. The effects of surface modified c-MWCNT have been investigated in terms of the thermal, rheological, and mechanical properties of TLCP/c-MWCNT nanocomposites.

EXPERIMENTAL

Materials and preparation of composites

The TLCP used in this research was Zenite 6000 (Dupont), which is wholly aromatic polyester.[24] The CNT used as a nanoreinforcement is MWCNT (purity $>$ 95%) synthesized from a thermal chemical vapor deposition process, purchased from Iljin Nanotech, Korea. The MWCNT has the diameter of 10–40 nm, and their aspect ratio is $\sim$ 1000. All materials were dried at 120°C *in vacuo* for at least 24 h, before use to eliminate the effect of moisture. The carboxylated MWCNT (c-MWCNT) was prepared according to conventional method by following process: the MWCNT was treated with a mixture of concentrated H_2SO_4 and HNO_3 in a ratio 3 : 1 at 70°C for 2 h, and the mixture was sonicated for 1 h at sonication bath. Then the mixture was washed with distilled water and filtered through a membrane filter made of poly(tetra-fluoroethylene) until residual acid was not shown. The TLCP/c-MWCNT nanocomposites were prepared by melt compounding in a Haake rheometer (Gebr. Haake GmbH, Germany) equipped with a twin screw. The temperatures of heating zone, from the hopper to the die, were set to 320, 350, 360, and 360°C, and the screw speed was fixed at 25 rpm. For fabrication of TLCP/c-MWCNT nanocomposites, the c-MWCNT contents were 0.01, 0.05, 0.l, and 0.2 wt % in the TLCP matrix. The specimens for mechanical test were prepared by 55-ton vertical injection molding machine (Wonil Hydraulic, Korea).

Characterization

The c-MWCNT was characterized using Raman spectrometer (NRS-3100, Jasco, Japan) and Fourier transform infrared spectrometer (Magna-IR. 760 ESP, Nicolet). Thermogravimetric analysis (TGA) of TLCP/c-MWCNT nanocomposites was performed with a TA Instrument SDT-2960 TGA under nitrogen over the temperature range of 30–900°C at a heating rate of 10°C/min. Differential scanning calorimetry (DSC) analysis of TLCP/c-MWCNT nanocomposites was carried out using a PerkinElmer DSC 7 over the temperature range of 30–350°C at a scan rate of 10°C/min. The mechanical properties of nanocomposites were investigated at room temperature using an Instron 4465 and 3367 testing machine according to the procedures in the ASTM D 638 and ASTM D 790 standard, respectively. The values of the mechanical properties used in this research represented the average over at least five individual measurements. Heat deflection temperature (HDT) of TLCP/c-MWCNT nanocomposites was measured under load of 1.8 MPa according to the ASTM D 648 standard. The morphology of the fractured surfaces of TLCP/c-MWCNT nanocomposites was observed using a field emission (FE-SEM, JEOL, JSM-6330F). The rheological properties of the melt state of the TLCP/c-MWCNT nanocomposites were measured at 350°C with an advanced rheometric expansion system (ARES, Rheometric Scientific). The dynamic shear measurements were performed in oscillation mode, and parallel plate geometry with a diameter of 25 mm was used. The plate gap was 1 mm, and frequency sweep measurements were conducted over the angular frequency range of 0.05–500 rad/s within linear viscoelastic range.

RESULTS AND DISCUSSION

Confirmation of surface treatment

To confirm the surface treatment of the MWCNT, the Raman and FTIR were used. The Raman spectra of the MWCNT and c-MWCNT are shown in Figure 1. The Raman spectra of the MWCNT and c-MWCNT exhibited two characteristic peaks around 1350 and 1585 cm^{-1}. The peak near 1350 cm^{-1} (D band) is attributed the disordered carbon atom, and the peak observed at near 1585 cm^{-1} (G band) reflects the structural intensity of the sp^2-hybridized carbon atoms, corresponding to the graphite E_{2g} vibrational modes, respectively.[25–27] The Raman spectra curve of MWCNT before and after acid treatment exhibited the same pattern, and the ratios of I_D/I_G of c-MWCNT are almost same to those of pristine MWCNT. This implies that the bonding structure of the walls of the CNT was not damaged by this acid treatment. The FTIR spectra of the MWCNT and c-MWCNT are shown in Figure 2. The peaks observed at $\sim$ 1630 and 1570 cm^{-1} in curve of the MWCNT and c-MWCNT were corresponded to the

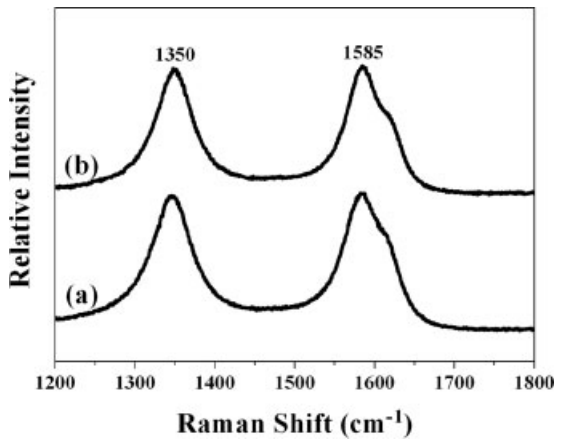

Figure 1 Raman spectra of (a) pristine MWCNT and (b) c-MWCNT.

C=C stretching vibrations of CNT, which was caused by inherent structure of CNT. The peaks observed at ~ 1720 and 1220 cm^{-1} were corresponded to the C=O and C—O stretching vibrations of the carboxylic acid groups, respectively, indicating that the carboxylic groups were attached on the surface of the c-MWCNT through the acid treatment of the MWCNT.[28]

Thermal properties

Thermal behaviors of TLCP/c-MWCNT nanocomposites investigated by DSC are shown in Table I. The glass transition temperatures (T_g) of TLCP and TLCP/c-MWCNT were not observed. In addition, incorporation of small amount of c-MWCNT into TLCP matrix had little effect on the melting temperature (T_m) and crystallization temperature (T_c) of the TLCP/c-MWCNT nanocomposites, and the degree of supercooling was not changed as c-MWCNT is incorporated into the TLCP. Many researches[21–23,29–31] have reported that MWCNT enhanced the nucleation of crystallization for polymer/MWCNT nanocomposites. However, c-MWCNT could not effectively act as nucleating agents in the TLCP/c-MWCNT nanocomposites. In general, crystallization of the TLCP is considerably different from that of other conventional polymers.[24] The molecules of TLCP are rigid compared with conventional polymer, which implies that larger translations of TLCP molecules are required for recrystallization.[12,32,33] In addition, crystallization of TLCP occurs so rapidly on cooling that the process of quenching from nematic liquid crystalline to glassy state results in some crystallization.[34] Therefore, it is suggested that small amount of c-MWCNT could not effectively act as nucleating agent because of these properties for crystallization of TLCP. And also, it could be explained that c-MWCNT may be not nucleating material to enhance the nucleation of crystallization of TLCP in this TLCP/c-MWCNT nanocomposites.

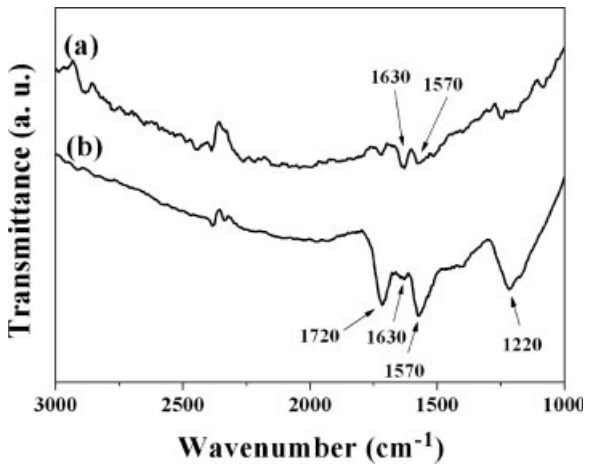

Figure 2 FTIR spectra of (a) pristine MWCNT and (b) c-MWCNT.

The parameters to evaluate thermal stability of the TLCP/c-MWCNT nanocomposites from the TGA thermogram are shown in Table II. The thermal decomposition temperature at the maximum rate (T_{dm}), residual yield (W_R) and integral procedural decomposition temperature (IPDT) were evaluated to determine thermal stability of TLCP/c-MWCNT nanocomposites. The schematic TGA thermogram for determining the IPDT of polymer nanocomposites based on the Doyle's proposition[35] is shown in Figure 3,[36] and then the IPDT is calculated as follows:

$$\text{IPDT } (^\circ\text{C}) = A^* K^* \ (T_f - T_i) + T_i \qquad (1)$$

$$A^* = \frac{A_1 + A_2}{A_1 + A_2 + A_3} \quad \text{and} \quad K^* = \frac{A_1 + A_2}{A_1}$$

where, A^* is area ratio of the total experimental curve divided by the total TGA thermogram; K^* is

TABLE I
DSC Results for TLCP and TLCP/c-MWCNT Nanocomposites at a Cooling Rate of 10°C/min

Material	T_c (°C)[a]	ΔH_c (J/g)[a]	T_m (°C)[b]	ΔT (°C)[c]
TLCP	291.7	1.546	332.0	40.3
TLCP/c-MWCNT 0.01	291.2	1.378	335.0	43.8
TLCP/c-MWCNT 0.1	290.9	0.976	333.1	42.2
TLCP/c-MWCNT 0.2	289.3	0.543	331.3	42.0

[a] The crystallization temperature obtained from cooling at 10°C/min.
[b] The melting temperature obtained from heating at 10°C/min.
[c] Degree of supercooling, $\Delta T = T_m - T_c$.

TABLE II
Thermal Stability of TLCP/c-MWCNT Nanocomposites with Different c-MWCNT Content

Materials	T_{dm}[a] (°C)	W_R[b] (°C)	A^*	K^*	A^*K^*	IPDT (°C)
TLCP	533.2	20.4	0.719	1.399	1.006	905.0
TLCP/c-MWCNT 0.01	534.0	22.7	0.731	1.452	1.062	954.0
TLCP/c-MWCNT 0.1	535.3	24.4	0.739	1.498	1.107	992.8
TLCP/c-MWCNT 0.2	539.4	30.1	0.762	1.629	1.241	1108.7

[a] Decomposition temperature at the maximum decomposition rate.
[b] Residual yield in TGA at 900°C under nitrogen.

the coefficient of A^*; T_i is the initial experimental temperature (°C), and T_f is the final experimental temperature (°C). The values of T_{dm} and W_R as well as IPDT increased with increasing c-MWCNT content, which indicates that the incorporation of c-MWCNT enhanced the thermal stability of TLCP/c-MWCNT nanocomposites. The enhancement of thermal stability for the TLCP/c-MWCNT nanocomposites may be attributed to a physical barrier effect of the MWCNT, which prevented the transport of decomposition in the polymer nanocomposites.[37,38] Similar results that MWCNT hindered the transport of degradation in the composites system are observed at PEN/MWCNT and PET/MWCNT nanocomposites.[22,23] Therefore, it could be demonstrated that a very small amount of c-MWCNT acted as effective thermal degradation resistant reinforcements in the TLCP matrix, enhancing the thermal stability of the TLCP/c-MWCNT nanocomposites.

Rheological properties

The complex viscosity of TLCP/c-MWCNT nanocomposites at 350°C as a function of frequency is shown in Figure 4. The complex viscosity of TLCP/c-MWCNT nanocomposites decreased with increasing frequency, indicating a non-Newtonian behavior over the frequency range investigated. The shear-thinning behavior of TLCP/c-MWCNT nanocomposites resulted from the high-shear thinning characteristic of TLCP by the orientation of the rigid molecular chains during the applied shear force. To investigate the effect of c-MWCNT content on the complex viscosity of TLCP/c-MWCNT nanocomposites, the complex viscosity of nanocomposites at different frequency is shown in Figure 5. Incorporation of the c-MWCNT into the TLCP matrix had a slight effect on the complex viscosity of TLCP/c-MWCNT nanocomposites. In general, melt viscosity of the composites increases with filler content, which decreases the processability of filled system polymer composites. However, the extent of increase in the complex viscosity of TLCP/c-MWCNT nanocomposites with c-MWCNT content was small. Therefore, it is very remarkable that the processability of TLCP/c-MWCNT nanocomposites was not decreased by incorporation of c-MWCNT into the TLCP, which makes it possible to fabricate the high-performance polymer nanocomposites with good processability.

The storage modulus of TLCP/c-MWCNT nanocomposites as a function of the frequency is shown in Figure 6. The storage modulus of TLCP/c-MWCNT nanocomposites increased with increasing frequency and was higher than that of pure TLCP. In addition, the storage modulus of the TLCP/c-MWCNT nanocomposites increased with increasing c-MWCNT content, as shown in Figure 7. This result

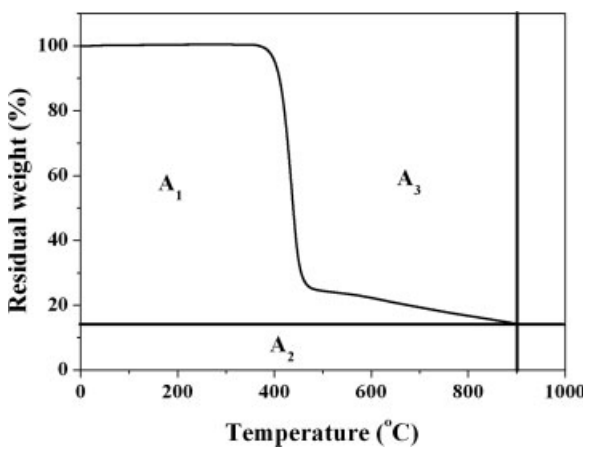

Figure 3 Schematic TGA thermogram to determine the IPDT.

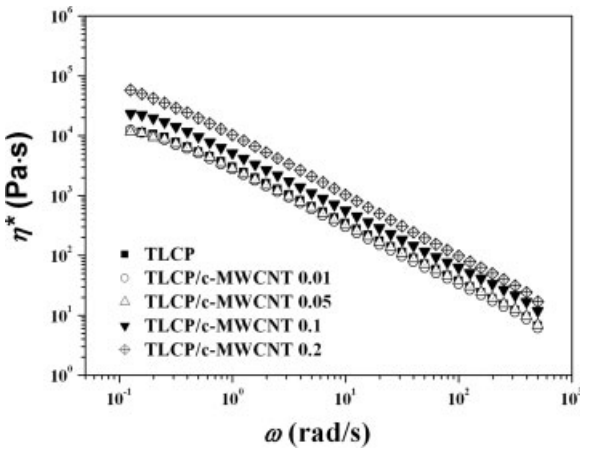

Figure 4 Variations of complex viscosity of TLCP/c-MWCNT nanocomposites with c-MWCNT content as a function of frequency.

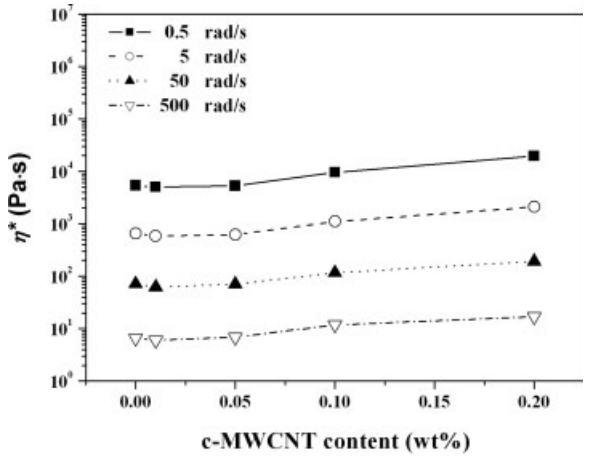

Figure 5 Variations of the complex viscosity of TLCP/c-MWCNT nanocomposites at different frequencies with c-MWCNT contents.

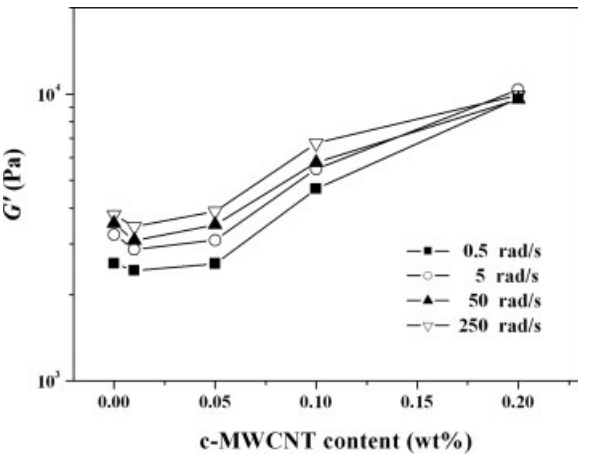

Figure 7 Variations of storage modulus of TLCP/c-MWCNT nanocomposites at different frequencies with c-MWCNT content.

can be explained by the fact that the physical interaction between the nanotubes could lead to the formation of an interconnected or network-like structures of the nanotubes in the polymer matrix as the c-MWCNT content increased.[39] And also, this result was similar to the tendency observed in the complex viscosity of TLCP/c-MWCNT nanocomposites with increasing c-MWCNT content.

The shear-thinning exponent and relaxation exponent of the TLCP/c-MWCNT nanocomposites were characterized to investigate the effect of c-MWCNT on the rheological properties of TLCP/c-MWCNT nanocomposites. The shear-thinning exponent is the slope in the plot of complex viscosity versus frequency, and the relaxation exponent is the slope in the plot of storage modulus versus frequency.[40,41] An ideal non-Newtonian fluid has a shear thinning exponent that equals or approaches zero, and the viscosity is independent of frequency. The shear-thinning exponent and relaxation exponent of TLCP/c-MWCNT nanocomposites are shown in Table III. In general, the shear-thinning behavior significantly depends on the filler content in polymer/filler composites.[40–43] However, the extent of variation in the shear-thinning exponent of the TLCP/c-MWCNT nanocomposites was very small. This is because the shear-thinning behavior of TLCP/c-MWCNT nanocomposites depends on the matrix rather than the c-MWCNT content because of the very strong shear-thinning behavior of TLCP. The relaxation exponent of TLCP/c-MWCNT nanocomposites decreased with increasing c-MWCNT content, and the extent of decrease was more pronounced at higher c-MWCNT content. This result demonstrates that nanotube–nanotube interactions dominate with increasing c-MWCNT content, leading to the formation of an interconnected structure or network-like of c-MWCNT in the TLCP/c-MWCNT nanocomposites.[43,44]

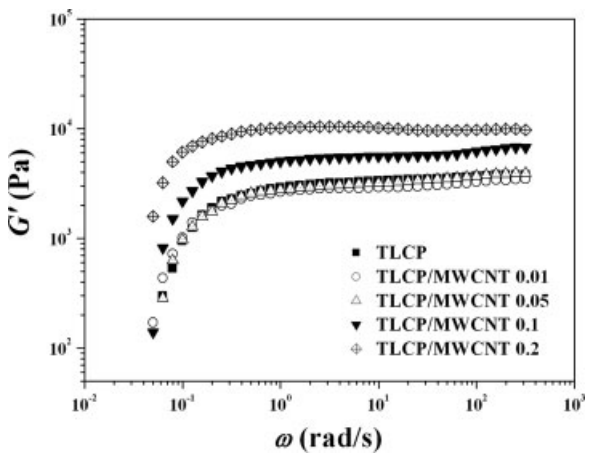

Figure 6 Variations of storage modulus of TLCP/c-MWCNT nanocomposites with c-MWCNT content as a function of frequency.

Mechanical properties and morphology

The mechanical properties of TLCP/c-MWCNT nanocomposites with c-MWCNT content are shown

TABLE III
Variations of the Shear-Thinning Exponent and Relaxation Exponent of the TLCP/c-MWCNT Nanocomposites with c-MWCNT Content

Materials	Shear-thinning exponent	Relaxation exponent
TLCP	−0.81	1.08
TLCP/MWCNT 0.01	−0.84	1.06
TLCP/MWCNT 0.05	−0.81	1.02
TLCP/MWCNT 0.1	−0.85	0.84
TLCP/MWCNT 0.2	−0.9	0.50

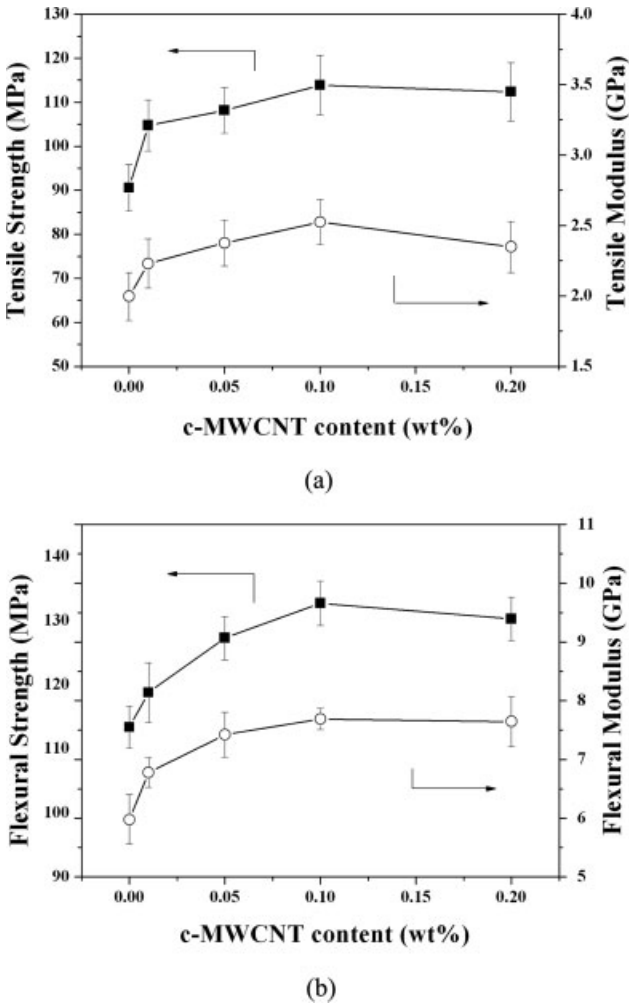

Figure 8 Variation of (a) tensile strength and modulus and (b) flexural strength and modulus of TLCP/c-MWCNT nanocomposites with c-MWCNT content.

in Figure 8. The mechanical properties of nanocomposites were improved as c-MWCNT content increased, which could be attributed to the effective reinforcement effect of c-MWCNT in the TLCP/c-MWCNT nanocomposites. There are four main system requirements for effective reinforcement: large aspect ratio, interfacial stress transfer, alignment, and good dispersion.[45] The c-MWCNT has high aspect ratio, which implies that the c-MWCNT could act effectively as reinforcement in the TLCP/c-MWCNT nanocomposites. In addition, the interfacial adhesion between TLCP matrix and c-MWCNT may be improved through the carboxylic acid group on the surface of c-MWCNT, which could lead to efficient load transfer to nanotube. Compared with conventional thermoplastics, TLCPs undergo spontaneous molecular alignment in the melt state due to the high rigidity of their chains, which leads to their excellent physical properties.[15] Therefore, alignment of c-MWCNT with spontaneous alignment of TLCP molecules could give rise to significant enhancement in mechanical properties of TLCP/c-MWCNT nanocomposites. However, c-MWCNT could prevent the spontaneous molecular alignment of TLCP as the c-MWCNT content increased, which may lead that the improvement in mechanical properties of nanocomposites was not increased at 0.2 wt % c-MWCNT content.

The HDT is considered as the upper temperature limit to use the material which service at a certain period, and it provides important information for product design, including the service temperature of final products.[46–48] Variation of the HDT for the TLCP/c-MWCNT nanocomposites as a function of c-MWCNT content is shown in Figure 9. The HDT of TLCP/c-MWCNT nanocomposites was increased with increasing c-MWCNT content, and this result is similar to those of other mechanical properties such as tensile and flexural properties of TLCP/c-MWCNT nanocomposites. The variation of the HDT was related to the behavior of flexural modulus with filler content.[46] The improvement in the HDT of the TLCP/c-MWCNT nanocomposites was attributed to the improvement in the flexural modulus with c-MWCNT contents. This result can be explained by the fact that incorporation of the c-MWCNT into the TLCP could increase the stiffness and ability of nanocomposites to retain stiffness with increasing temperature.

A good dispersion of CNT in the polymer matrix is one of the most important and challenging tasks to fabricate the high-performance polymer/CNT nanocomposites, because homogeneous and uniform dispersion of CNT makes it possible to transfer load to the nanotube efficiently in the polymer nanocomposites. Scanning electron microscope (SEM) images of fractured surface of TLCP, TLCP/pristine-MWCNT, and TLCP/c-MWCNT nanocomposites are

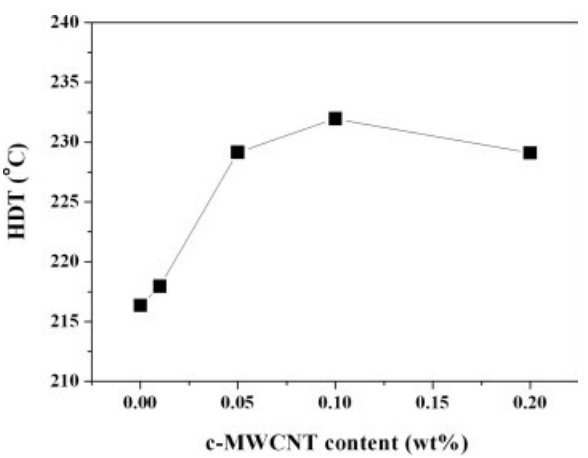

Figure 9 Variation of the HDT of TLCP/c-MWCNT nanocomposites with c-MWCNT content.

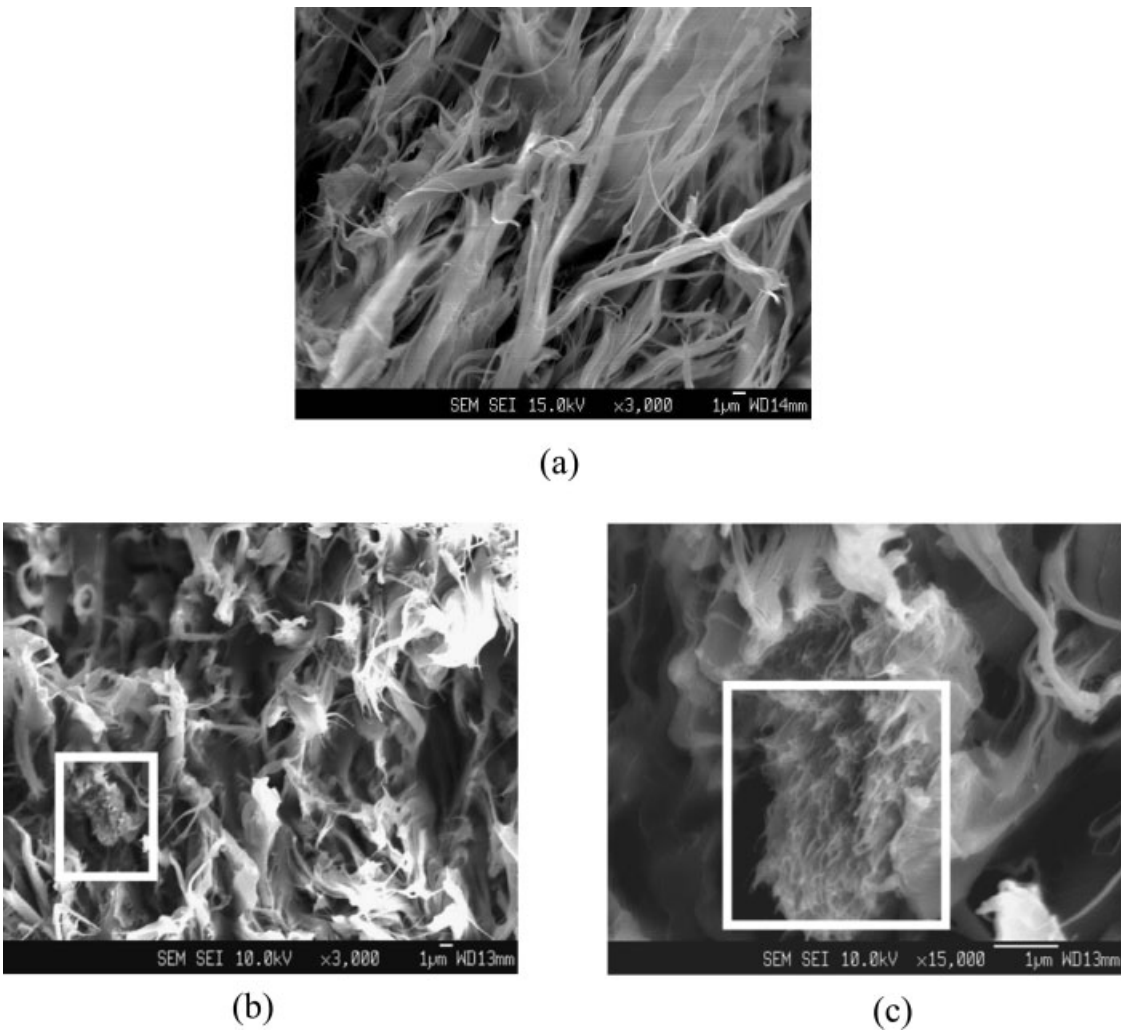

Figure 10 SEM images of fracture surfaces of (a) neat TLCP, (b) TLCP/c-MWCNT nanocomposites, and (c) enlarged SEM image of selected region in (b).

shown in Figures 10 and 11. As shown in Figure 10(a), TLCP has highly orientated structure and continuous microfibrils, which lead to excellent mechanical properties. In addition, this unique structure of the TLCP results in an improvement in the mechanical properties of conventional polymer composites reinforced with TLCP and the high-mechanical anisotropy of TLCP. Agglomerated MWCNT was observed in the TLCP/pristine-MWCNT nanocomposites as shown in Figure 10(b,c) at the highlighted box area. In general, CNTs often tend to bundles together by van der Waals interaction between the individual nanotubes with high aspect ratio and large surface area and lead to some agglomerations, which prevent efficient load transfer to nanotube.[49] Furthermore, the agglomerations of CNTs in the nanocomposites can act as weak point when an external force is imposed in the nanocomposites, which may be the cause of the stress concentration phenomena.[22] As a result, mechanical properties were not improved in the TLCP/pristine-MWCNT nanocomposites because of some agglomerated structures of pristine-MWCNT dispersed in the nanocomposites.[50] As shown in Figure 11(a,b), c-MWCNTs were uniformly dispersed in the TLCP/c-MWCNT nanocomposites. This can be demonstrated that the van der Waals attraction may be reduced by carboxylic acid group on the outer wall of c-MWCNT. In addition, aligned c-MWCNT was observed in Figure 11(c), which deduces that c-MWCNT was aligned with spontaneous alignment of TLCP molecules in the TLCP/c-MWCNT nanocomposites. Therefore, the improvement in mechanical properties of TLCP/c-MWCNT nanocomposites may be resulted from the uniform dispersion and alignment of c-MWCNT in the TLCP matrix, leading to an efficient load transfer to the nanotube in the nanocomposites.

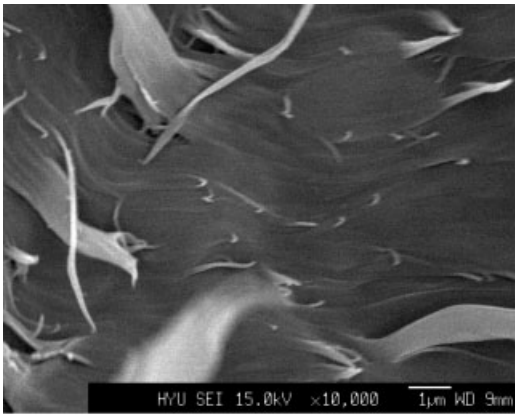

(a)

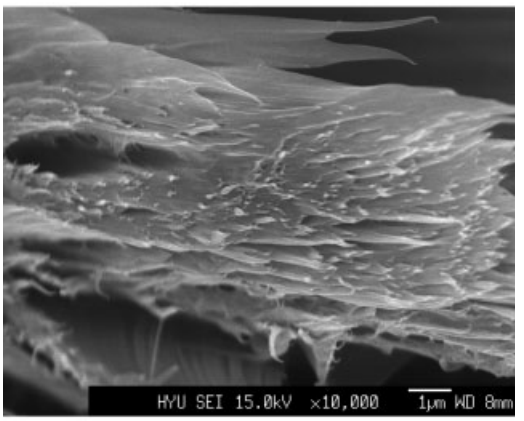

(b)

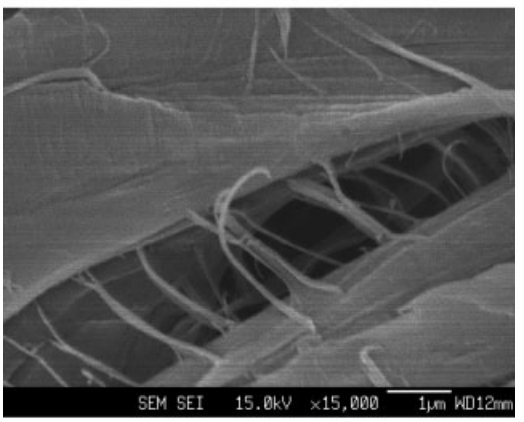

(c)

Figure 11 SEM images of fracture surfaces of TLCP/c-MWCNT nanocomposites containing 0.1 wt % of c-MWCNT.

CONCLUSIONS

The MWCNT was treated with mixture of concentrated acids to improve uniform dispersion of MWCNT in the polymer matrix and to obtain better interfacial adhesion between MWCNT and polymer matrix. The bonding structure of the walls of the MWCNT was not damaged, and the carboxylic groups were attached on the surface of the MWCNT through the acid treatment. TLCP/c-MWCNT nanocomposites were prepared by a melt-compounding process in twin-screw extruder, and thermal, rheological, and mechanical properties of nanocomposites were investigated. Incorporation of c-MWCNT into the TLCP matrix had little effect on the crystallization of TLCP, which indicates that the c-MWCNT may be not nucleating material to enhance the nucleation of crystallization of TLCP. However, thermal stability of TLCP/c-MWCNT nanocomposites was increased with c-MWCNT contents due to the physical barrier effect of c-MWCNT in the nanocomposites. The incorporation of c-MWCNT has a slight effect on the complex viscosity of TLCP/c-MWCNT nanocomposite, which indicates that it is possible to fabricate the high-performance polymer nanocomposites with good processability. The slope of the plot of storage modulus versus frequency at terminal zone was decreased with c-MWCNT content, which may be attributed that some interconnected or network-like structure of c-MWCNT was formed in the TLCP/c-MWCNT nanocomposites as c-MWCNT content increased. The mechanical properties of TLCP/c-MWCNT nanocomposites were improved by the incorporation of small amount of c-MWCNT, which implies that even very small amount of c-MWCNT could act effectively as reinforcement in the TLCP/c-MWCNT nanocomposites. This was attributed to the uniform dispersion of c-MWCNT in the TLCP/c-MWCNT nanocomposites.

References

1. Iijima, S. Nature 1991, 354, 56.
2. Nalwa, H. S. Handbook of Nanostructured Materials and Nanotechnology, Vol. 5; San Diego: Academic Press, 1994; pp 399–410.
3. Ajayan, P. M.; Stephan, O.; Colliex, C.; Trauth, D. Science 1994, 265, 1212.
4. Ago, H.; Petritsch, K.; Shaffer, M. S. P.; Windle, A. H.; Friend, R. H. Adv Mater 1999, 11, 1281.
5. Goh, H. W.; Goh, S. H.; Xu, G. Q.; Lee, K. Y.; Yang, G. Y.; Lee, Y. W.; Zhang, W. D. J Phys Chem B 2003, 107, 6056.
6. Watts, P. C. P.; Hsu, W. K.; Kroto, H. W.; Walton, D. R. M. Nano Lett 2003, 3, 549.
7. Zhang, W. D.; Shen, L.; Phang, I. Y.; Liu, T. Macromolecules 2004, 37, 256.
8. Sun, Y. P.; Fu, K.; Lin, Y.; Huang, W. Acc Chem Res 2002, 35, 1096.
9. Bellayer, S.; Gilman, J. W.; Eidelman, N.; Bourbigot, S.; Flambard, X.; Fox, D. M.; De Long, H. C.; Trulove, P. C. Adv Funct Mater 2005, 15, 910.
10. Bahr, J. L.; Tour, J. M. J Mater Chem 2002, 12, 1952.
11. Eitan, A.; Jiang, K.; Dukes, D.; Andrews, R.; Schandler, L. S. Chem Mater 2003, 15, 3198.
12. Chung, T. S. Polym Eng Sci 1986, 26, 901.

13. Park, D. S.; Kim, S. H. J Appl Polym Sci 2003, 87, 1842.
14. Bretas, R. E. S.; Baird, D. G. Polymer 1992, 33, 5233.
15. Guerrica-Echevarria, G.; Eguiazàbal, J. I.; Nazàbal, J. J Appl Polym Sci 2003, 88, 998.
16. Andrews, R.; Jacques, D.; Qian, D.; Rantell, T. Acc Chem Res 2002, 35, 1008.
17. Jin, Z.; Pramoda, K. P.; Xu, G.; Goh, S. H. Chem Phys Lett 2001, 337, 43.
18. Manchado, M. A. L.; Valentini, L.; Biagiotti, J.; Kenny, J. M. Carbon 2005, 43, 1499.
19. Liu, T.; Phang, I. Y.; Shen, L.; Chow, S. Y.; Zhang, W. D. Macromolecules 2004, 37, 7214.
20. Pötschke, P.; Bhattacharyya, A. R.; Janke, A.; Goering, H. Compos Interf 2003, 10, 389.
21. Kim, J. Y.; Park, H. S.; Kim, S. H. Polymer 2006, 47, 1379.
22. Kim, J. Y.; Kim, S. H. J Polym Sci Part B: Polym Phys 2006, 44, 1062.
23. Kim, J. Y.; Park, H. S.; Kim, S. H. J Appl Polym Sci 2007, 103, 1450.
24. Pramoda, K. P.; Chung, T. S. Polym Eng Sci 2002, 42, 439.
25. Hiura, H.; Ebbesen, T. W.; Tanigaki, K.; Takahashi, H. Chem Phys Lett 1993, 202, 509.
26. Li, W.; Zhang, H.; Wang, C.; Zhang, Y.; Xu, L.; Zhu, K.; Xie, S. Appl Phys Lett 1997, 70, 2684.
27. Liu, Y.; Pan, C.; Wang, J. J Mater Sci 2004, 39, 1091.
28. Zhao, C.; Ji, L.; Liu, H.; Hu, G.; Zhang, S.; Yang, M.; Yang, Z. J Solid State Chem 2004, 177, 4394.
29. Wang, B.; Sun, G.; Liu, J.; He, X.; Li, J. J Appl Polym Sci 2006, 100, 3794.
30. Assouline, E.; Lustiger, A.; Barber, A. H.; Cooper, C. A.; Klein, E.; Wachtel, E.; Wagner, H. D. J Polym Sci Part B: Polym Phys 2003, 41, 520.
31. Funck, A.; Kaminsky, W. Compos Sci Technol 2007, 67, 906.
32. Economy, J.; Goranov, K. Adv Polym Sci 1994, 117, 221.
33. Jaffe, M.; Menczel, J. D.; Bessey, W. E. Thermal Characterization of Polymeric Materials, 2nd ed.; Academic Press: San Diego, 1997; Chapter 2.
34. Butzbach, G. D.; Wendorff, J. H.; Zimmerman, H. J. Makromol Chem Rapid Commun 1985, 6, 821.
35. Doyle, C. D. Anal Chem 1961, 33, 77.
36. Park, S. J.; Cho, M. S. J Mater Sci 2000, 35, 3525.
37. Kashiwagi, T.; Grulke, E.; Hilding, J.; Harris, R.; Awad, W.; Douglas, J. Macromol Rapid Commun 2002, 23, 761–765.
38. Kashiwagi, T.; Shields, J. R.; Harris, R. H.; Davis, R. D. J Appl Polym Sci 2003, 87, 1541.
39. Seo, M. K.; Park, S. J. Chem Phys Lett 2004, 395, 44.
40. Wagener, R.; Reisinger, T. J. G. Polymer 2003, 44, 7513.
41. Costa, F. R.; Wagenknecht, U.; Jehnichen, D.; Abdel-Goad, M.; Heinrich, G. Polymer 2006, 47, 1649.
42. Krishnamoorti, R.; Vaia, R. A.; Giannelis, E. P. Chem Mater 1996, 8, 1728.
43. Abdel-Goad, M.; Pötschke, P. J Non-Newtonian Fluid Mech 2005, 128, 2.
44. Kim, J. A.; Seong, D. G.; Kang, T. J.; Youn, J. R. Carbon 2006, 44, 1898.
45. Coleman, J. N.; Khan, U.; Blau, W. J.; Gun'ko, Y. K. Carbon 2006, 44, 1624–1652.
46. Nielsen, L. E. Mechanical Properties of Polymers and Composites, Vol. 2; Marcel Dekker: New York, 1974; Chapter 6.
47. Wong, A. C. Y. Compos B 2003, 34, 199.
48. Kim, J. Y.; Kang, S. W.; Kim, S. H. Fibers Polym 2006, 7, 358.
49. Thess, A.; Lee, R.; Nikolaev, P.; Dai, H.; Petit, P.; Robert, J.; Xu, C.; Lee, Y. H.; Kim, S. G.; Rinzler, A. G.; Colbert, D. T.; Scuseria, G. E.; Tomanek, D.; Fisher, J. E.; Smalley, R. E. Science 1996, 273, 483.
50. Park, S. K.; Kim, S. H.; Hwang, J. T. SPE ANTEC 2007, 49.